molecular oral microbiology

molecular oral microbiology

Fur homolog regulates *Porphyromonas gingivalis* virulence under low-iron/heme conditions through a complex regulatory network

J. Ciuraszkiewicz[1], M. Śmiga[1], P. Mackiewicz[2], A. Gmiterek[1], M. Bielecki[1], M. Olczak[1] and T. Olczak[1]

1 Laboratory of Biochemistry, Faculty of Biotechnology, University of Wroclaw, Wroclaw, Poland
2 Department of Genomics, Faculty of Biotechnology, University of Wroclaw, Wroclaw, Poland

Correspondence: Teresa Olczak, Laboratory of Biochemistry, Faculty of Biotechnology, University of Wroclaw, 14A. F. Joliot-Curie St., 50-383 Wroclaw, Poland Tel.: +48 71 3752612; fax: +48 71 3752608; E-mail: Teresa.Olczak@biotech.uni.wroc.pl

Keywords: Fur; gingipain; hemagglutinin; HmuY; periodontitis; phylogeny; *Porphyromonas gingivalis*; virulence
Accepted 30 July 2014
DOI: 10.1111/omi.12077

SUMMARY

Porphyromonas gingivalis **is a key pathogen responsible for initiation and progression of chronic periodontitis. Little is known about the regulatory mechanisms of iron and heme uptake that allow *P. gingivalis* to express virulence factors and survive in the hostile environment of the oral cavity, so we initiated characterization of a *P. gingivalis* Fur homolog (PgFur). Many Fur paralogs found in microbial genomes, including Bacteroidetes, confirm that Fur proteins have a tendency to be subjected to a sub- or even neofunctionalization process. PgFur revealed extremely high sequence divergence, which could be associated with its functional dissimilarity in comparison with other Fur homologs. A *fur* mutant strain constructed by insertional inactivation exhibited retarded growth during the early growth phase and a significantly lower tendency to form a homotypic biofilm on abiotic surfaces. The mutant also showed significantly weaker adherence and invasion to epithelial cells and macrophages. Transcripts of many differentially regulated genes identified in the *fur* mutant strain were annotated as hypothetical proteins, suggesting that PgFur can play a novel role in the regulation of gene expression. Inactivation of the *fur* gene resulted in decreased *hmuY* gene expression, increased expression of other *hmu* components and changes in the expression of genes encoding hemagglutinins and proteases (mainly gingipains), HtrA, some extracytoplasmic sigma factors and two-component systems. Our data suggest that PgFur can influence *in vivo* growth and virulence, at least in part by affecting iron/heme acquisition, allowing efficient infection through a complex regulatory network.**

INTRODUCTION

Periodontal diseases are among the most common chronic infections in humans (Graves *et al.*, 2000; Craig *et al.*, 2003; Hajishengallis, 2011). From the clinical point of view, periodontitis is characterized by deep periodontal pockets resulting from the loss of connective tissue attachment and alveolar bone, which is caused by destructive activity of bacterial agents, such as proteolytic enzymes (Potempa *et al.*, 2003). The severity of the bleeding on probing depends on the intensity of the gingival inflammation (Craig *et al.*, 2003; Nakagawa *et al.*, 2006). Analyses of bacterial species isolated from subgingival samples revealed the presence and relative abundance of periodontal pathogens, including the 'red complex' bacteria (*Porphyromonas gingivalis*, *Tannerella forsythia* and *Treponema denticola*), associated with the clinical

© 2014 John Wiley & Sons A/S. Published by John Wiley & Sons Ltd

features of chronic periodontitis (Griffen *et al.*, 1998; Haffajee *et al.*, 1998; Gmiterek *et al.*, 2013). Among them, *P. gingivalis* (gram-negative, black-pigmented, anaerobic bacterium) is considered the main etiological agent and a key pathogen responsible for initiation and progression of chronic periodontitis (Bostanci & Belibasakis, 2012). In the natural environment, *P. gingivalis* is a constituent of a mixed-species biofilm that exists in the oral cavity (Marsh, 2004; Kuboniwa & Lamont, 2010). The bacterium can enter gingival epithelial and immune cells and remain viable and capable of spreading among host cells, so contributing to its survival in the oral cavity (Lamont *et al.*, 1995; Vitkov *et al.*, 2005; Yilmaz *et al.*, 2006; Guyodo *et al.*, 2012). The *P. gingivalis* does not produce and use siderophores to gain iron and is absolutely dependent on heme, as the sole source of iron and protoporphyrin IX (Olczak *et al.*, 2005). The availability of iron in mammalian cells is very low, mainly because of its sequestration by iron-binding proteins. Also, heme is not readily available in the host and the majority of this molecule is bound by hemoglobin, hemopexin and serum albumin. On the other hand, higher concentrations of iron and heme can be toxic, as both compounds are able to catalyse the generation of free radicals, promoting cellular damage and oxidative stress. To overcome these significant problems, microorganisms evolved sophisticated mechanisms of iron homeostasis.

Regulation of gene expression in bacteria is usually performed at the transcriptional level by the specific action of DNA-binding proteins and at the post-transcriptional level by specific protein–protein interactions (Hantke, 2001). Among the best characterized bacterial regulators there is a ferric uptake regulator (Fur), which can regulate the expression of genes in response to iron concentration through several different mechanisms. In the classical Fur regulation paradigm, under high-iron conditions, Fur becomes ferrated and binds to specific Fur box sequences located in promoters of regulated genes, thereby preventing their transcription through steric hindrance of RNA polymerase. Under iron-restricted conditions, the Fur–Fe^{2+} complex dissociates and the repressor becomes inactive, which leads to transcription of target genes. In contrast to iron-dependent DNA-binding activity, Fur in some systems can sense signals other than iron or bind to DNA in the absence of a metal cofactor (Dubrac & Touati, 2000; Delany *et al.*, 2001), and Fur in some bacteria can bind heme (Hernandez *et al.*, 2004), which in turn can regulate Fur expression (Pellicer *et al.*, 2012). Importantly, it has been well documented that Fur functions as a global regulator that controls not only the expression of iron acquisition systems, but also a large number of genes involved in different cellular processes, such as stress response and production of virulence factors (Lee & Helmann, 2007). Tertiary structure, determined for Fur proteins from *Pseudomonas aeruginosa* (Pohl *et al.*, 2003), *Vibrio cholerae* (Sheikh & Taylor, 2009), *Helicobacter pylori* (Dian *et al.*, 2011) and *Campylobacter jejuni* (Butcher *et al.*, 2012), and for the DNA-binding domain from *Escherichia coli* Fur (Pecqueur *et al.*, 2006), showed that the Fur protein possesses two domains connected by a hinge loop: an N-terminal DNA-binding domain with a winged-helix motif and a C-terminal dimerization domain.

To acquire iron and heme, *P. gingivalis* uses several sophisticated mechanisms (Olczak *et al.*, 2005; Benson & Rivera, 2013), and some of them, notably the *hmu* system (Olczak *et al.*, 2008; Wojtowicz *et al.*, 2009, 2013; Smalley *et al.*, 2011; Byrne *et al.*, 2013) and gingipain proteases (Potempa *et al.*, 2003), are well characterized. The *P. gingivalis hmu* operon encodes hemophore-like lipoprotein (HmuY; PG1551), TonB-dependent outer-membrane receptor (HmuR; PG1552) and four hypothetical proteins of unknown function (PG1553–PG1556). Proteolytic activity of *P. gingivalis* is caused mainly by a group of cysteine proteases, comprising secreted and membrane-associated gingipains. Arginine-specific gingipains (RgpA and RgpB) are encoded by the *rgpA* and *rgpB* genes, and lysine-specific gingipain (Kgp) by the *kgp* gene. The predominant form of Kgp and RgpA is a complex of a catalytic domain with hemagglutinin/adhesion (Hag) domains. Although several mechanisms of uptake of iron, heme and other nutrients are well characterized, very little is known about regulatory mechanisms that allow *P. gingivalis* to survive in the very hostile environment of the oral cavity, a typical habitat characterized by low iron and heme concentrations. Given the high prevalence of chronic periodontitis, evidence for an association between periodontal infections and systemic conditions, such as diabetes mellitus, rheumatoid arthritis, cardiovascular and respiratory diseases (Meurman *et al.*, 2004; Rosenstein *et al.*, 2004), as well as increasing resistance of bacteria against antibiotics, and characterization of basic

© 2014 John Wiley & Sons A/S. Published by John Wiley & Sons Ltd

processes occurring in *P. gingivalis* is of high importance. Therefore, the aim of this study was to initiate characterization of a putative *P. gingivalis* Fur homolog (PgFur) with regard to its role played in iron/heme acquisition and virulence of this pathogen.

METHODS

Bacterial strains, growth conditions and biofilm formation

Porphyromonas gingivalis wild-type (A7436) and *fur* mutant (TO6) strains were grown anaerobically at 37°C for 3 days on blood agar plates (Biocorp, Warsaw, Poland) as described previously (Olczak *et al.*, 2008). These cultures were used as the inoculum for growth in liquid basal medium comprising 3% trypticase soy broth (Biocorp), supplemented with 0.5% yeast extract (Biocorp), 0.05% cysteine, 0.5 mg l^{-1} menadione (BM) and 5 mg l^{-1} hemin (BM+Hm). To mimic low-iron/heme conditions, bacteria were grown in the absence of heme and in the presence of an iron chelator, 160 μM 2,2-dipyridyl (BM+DIP). TO6 mutant strain was maintained in the presence of 1 μg ml^{-1} erythromycin. Bacterial growth was determined by measuring optical density (OD) at 600 nm. Homotypic biofilm formation was analysed using microplate assay and crystal violet staining as described previously (Olczak *et al.*, 2010).

Porphyromonas gingivalis fur mutant construction

The *P. gingivalis fur* gene (gene ID: 2551442; locus ID: PG0465) was inactivated by introducing the *ermF* cassette from *Bacteroides fragilis* to yield a *fur-ermF-fur* DNA fragment. Briefly, the *fur* gene was amplified from *P. gingivalis* genomic DNA using primers listed in Table 1 and cloned into the *Sal*I and *Hin*dIII restriction sites of the pGEM-3Zf(−) vector (Promega, Madison, WI). Then, a *B. fragilis ermF* encoding an erythromycin resistance gene was amplified from a pWS1 plasmid (Simpson *et al.*, 2000) and cloned into the native *Bgl*II restriction site of the *fur* gene. The resulting plasmid was introduced into *P. gingivalis* A7436 wild-type strain by electroporation. All constructs and homologous recombinations between the constructs and the chromosomal DNA of *P. gingivalis* were verified by polymerase chain reaction (PCR) and sequencing analyses (data not shown).

Cell culture invasion assay

Human histiocytic lymphoma cells (U937) and human acute monocytic leukemia cells (THP-1) cells were grown in RPMI-1640 medium (Cytogen GmbH, Sinn, Germany), supplemented with 10% heat-inactivated fetal bovine serum (Cytogen), 2 mM L-glutamine, 100 U ml^{-1} penicillin and 100 μg ml^{-1} streptomycin in a humidified atmosphere of 95% air and 5% CO_2 at 37°C. U937 cells were seeded at 0.3×10^6 ml^{-1} and subsequently stimulated to differentiate towards macrophages by treatment with 0.01 μg ml^{-1} phorbol 12-myristate 13-acetate (PMA, Sigma, St Louis, MO) for 48 h. The number and extent of differentiation of U937 cells were determined using Handheld Automated Cell Counter Scepter (Millipore, Billerica, MA). Fresh culture medium lacking antibiotics was added 24 h before inoculation with *P. gingivalis*. Similar experiments were carried out using THP-1 cells with the exception that PMA was used throughout the entire experiment. Human cervical epithelial HeLa cells (CCL-2) were cultured as described previously (Olczak *et al.*, 2012).

Bacteria were grown to the early stationary phase in BM+Hm as described above, collected by centrifugation at 10,000 ***g*** for 10 min at 4°C, washed three times with 20 mM sodium phosphate buffer, pH 7.4, containing 140 mM NaCl (PBS), and adjusted to an OD_{600} of 0.35. Viable bacterial cells (3.5×10^8 colony-forming units per ml) were added to host cells (0.35×10^6 cells ml^{-1} $well^{-1}$) seeded in fresh media without antibiotics at a multiplicity of infection (MOI) of 100 and incubated for 1, 4 and 24 h at 37°C in the presence of 5% CO_2. After removal of the culture media and their collection, cells were washed three times with PBS and aliquots of the cells were lysed with distilled water and collected. Medium containing gentamicin (300 μg ml^{-1}) and metronidazole (200 μg ml^{-1}) was then added to the remaining cells, and the cells were incubated for 60 min at 37°C in the presence of 5% CO_2 to kill extracellular bacteria. Then, the culture media were removed and the cells were washed three times with PBS, lysed and collected. Serial dilutions of culture media and cell lysates were plated on blood agar plates and *P. gingivalis* growth was determined using a colony-forming unit (ml) assay. All experiments were carried out in duplicate wells and repeated three times. Statistical analysis was performed using one-way analysis of

© 2014 John Wiley & Sons A/S. Published by John Wiley & Sons Ltd

Table 1 Primers designed and used in this study

Primer	5′→3′ sequence (restriction sites are underlined)	Product length (bp)	Locus ID and/or gene abbreviation	Description (reference)
FURMPR FURMPF	CTATGTCGACTCAAGGAGGATTCGCCCAC AGTCAAGCTTTGAAAGCGAGCGACAATATCG	797	PG0465, *fur*	Amplifies *P. gingivalis fur* gene with 5′ and 3′ flanking regions, adds *Sal*I (FURMPR) and *Hin*dIII (FURMPF) restriction sites (this study)
ERMFPR ERMBGL	ATCTAGATCTCTACGAAGGATGAAATTTTTCA TCAGAGATCTATCATAGAAATTGCATACCTTTG	1016	*ermF*	Amplifies *Bacteroides fragilis ermF* gene, adds *Bgl*II restriction sites at 5′ and 3′ ends (this study)
rtFUR6F rtFUR6R	TTCTGCGTTTGCCTTCTCCC TGAGATCCTTGTCGGCCAGT	191	PG0465, *fur*	Amplifies fragment of *P. gingivalis fur* gene, used in qRT-PCR (this study)
16SrRNA-F 16SrRNA-R	CTTGACTTCAGTGGCGGCAG AGGGAAGACGGTTTTCACCA	378	*16S rRNA*	Amplifies fragment of *P. gingivalis 16S rRNA* gene, used in qRT-PCR (Gmiterek *et al*., 2013)
rtTpr1F rtTpr1R	CTAAGACCCAAAGAGGGCAGG GAGGTCGTCGATGTCGAGTTT	137	PG1055, *tpr*	Amplifies fragment of *P. gingivalis tpr* gene, used in qRT-PCR (this study)
rtDcp2F rtDcp2R	GTTACGATACCTTCGCCCACT CTGTCGCTTTGGGCTTGTATG	111	PG1789, *dcp-2*	Amplifies fragment of *P. gingivalis dcp* gene, used in qRT-PCR (this study)
rtHem1F rtHem1R	CGCCGTATGACAATCCGATGA CCGAAGAGACACAGAGACCAC	150	PG1326	Amplifies fragment of *P. gingivalis* hemagglutinin gene, used in qRT-PCR (this study)
rtHagA2F rtHagA2R	AGGTGTACTTGGCATTCCGTC CGTGTACGTGTAGTCGTTGGA	107	PG1837, *hagA*	Amplifies fragment of *P. gingivalis hagA* gene, used in qRT-PCR (this study)
rtHagE2F rtHagE2R	ATACCGGCCGGAACTTATGAC TTCTTTCGTCGGTCCTTGTCC	87	PG2024, *hagE*	Amplifies fragment of *P. gingivalis hagE* gene, used in qRT-PCR (this study)
HYq4_F HYq4_R	GCTTCGAAATACGAAACGTG TATATCCGTCTGTCGGAACG	119	PG1551, *hmuY*	Amplifies fragment of *P. gingivalis hmuY* gene, used in qRT-PCR (Gmiterek *et al*., 2013)
FFURBsaIMVP RFURXhoI	GATCGGTCTCCCATGGTACCTTGGGCGATCT GATCCTCGAGTTATTTTTTCTTCTTGGGAGCGG	792	PG0465, *fur*	Amplifies sequence coding for untagged *P. gingivalis* Fur protein variant 1
FFURBsaIMDR RFURXhoI	GATCGGTCTCGCATGGATCGAAAAGATAAAAACCAA GATCCTCGAGTTATTTTTTCTTCTTGGGAGCGG	603	PG0465, *fur*	Amplifies sequence coding for untagged *P. gingivalis* Fur protein variant 2
FFURBsaIMIV RFURXhoI	GATCGGTCTCACATGATAGTCACATCACTGGAAG GATCCTCGAGTTATTTTTTCTTCTTGGGAGCGG	501	PG0465, *fur*	Amplifies sequence coding for untagged *P. gingivalis* Fur protein variant 3
FFURBsaIMVP RFURXhoIHis	GATCGGTCTCCCATGGTACCTTGGGCGATCT GATCCTCGAGTTTTTTCTTCTTGGGAGCGG	813	PG0465, *fur*	Amplifies sequence coding for 8His-tagged *P. gingivalis* Fur protein variant 1
FFURBsaIMDR RFURXhoIHis	GATCGGTCTCGCATGGATCGAAAAGATAAAAACCAA GATCCTCGAGTTTTTTCTTCTTGGGAGCGG	627	PG0465, *fur*	Amplifies sequence coding for 8His-tagged *P. gingivalis* Fur protein variant 2
FFURBsaIMIV	GATCGGTCTCACATGATAGTCACATCACTGGAAG	525	PG0465, *fur*	Amplifies sequence coding for 8His-tagged *P. gingivalis* Fur protein variant 3

Nucleotide sequences recognized by restriction enzymes are underlined.

© 2014 John Wiley & Sons A/S. Published by John Wiley & Sons Ltd

variance followed by Bonferroni's correction for multiple comparisons (GraphPad Software Inc., San Diego, CA). Differences with $P < 0.05$ were considered significant.

Porphyromonas gingivalis cell fractionation

Portions of bacterial cultures containing approximately 2×10^{10} cells were centrifuged at 10,000 ***g*** for 20 min at 4°C to separate the cell-free culture supernatant and cells. The pellets were gently washed once with cold PBS, then re-suspended in 1 ml of PBS with 10 mM *N*-α-*p*-tosyl-L-lysine chloromethyl ketone and kept frozen until used. The cells were disrupted using a UP100H sonicator (Hielscher Ultrasonics, Teltow, Germany) with 10 repeating 20-s bursts and 20-s intervals. Unbroken cells were removed by centrifugation at 20,000 ***g*** for 20 min at 4°C. The supernatant used as the whole-cell lysate fraction was subjected to ultracentrifugation at 150,000 ***g*** for 120 min at 4°C in a Beckman fixed-angle rotor (Type 70 Ti). Pelleted envelope fractions were re-suspended in 0.2 ml 10% sodium dodecyl sulfate (SDS) and incubated overnight at 16°C with continuous gentle mixing.

Sodium dodecyl sulfate–polyacrylamide gel electrophoresis

Total bacterial cell lysates were first analysed using SDS–polyacrylamide gel electrophoresis (PAGE) according to Laemmli (1970). In addition, the discontinuous SDS–PAGE procedure of Schagger (2006) was employed for determination of protein distribution using 9% or 13% gels. The amount of protein loaded per well was normalized against *P. gingivalis* culture volume and the number of cells was determined by measuring OD at 600 nm. Proteins were visualized by Coomassie Brilliant Blue G-250 (CBB) staining, which was preceded by overnight fixing in 0.1 M ammonium acetate in 50% methanol and 10% acetic acid.

Protein identification by mass spectrometry

Protein bands to be identified were excised from the gels, pooled and processed for mass spectrometry (MS) analysis according to the trypsin in-gel digestion procedure (Sigma Aldrich). Briefly, excised bands were incubated at 37°C for 30 min in 200 mM ammonium bicarbonate with 40% acetonitrile and then dried in a centrifugal vacuum concentrator Maxi dry lyo (Heto-Holten A/S, Allerod, Denmark). Proteins were subjected overnight to in-gel digestion with trypsin (8 μg ml^{-1}) in 40 mM ammonium bicarbonate and 9% acetonitrile solution at 37°C. Then, peptides were extracted from the gel for 30 min at 37°C with 0.1% trifluoroacetic acid in 50% acetonitrile solution, and concentrated using ZipTip (Millipore). Matrix-assisted laser-desorption ionization mass spectrometry (MALDI MS) was performed using a 4800 Plus MALDI time of flight (TOF)/TOF Analyzer (Applied Biosystems, Foster City, CA) on α-cyano-4-hydroxycinnamic acid as the matrix. The spectra were recorded within a mass range from 600 to 4000 Da at 200^{-1} laser frequency and power of 4500 AU. Proteomic analysis was carried out using MASCOT 2.3.0 software (www.matrixscience.com).

Microarray analysis

Total RNA was isolated (RNeasy Protect Bacteria Mini Kit, Qiagen, Hilden, Germany), RNA concentration and purity were determined (NanoDrop ND-1000 UV-Vis spectrophotometer, Peqlab, Erlangen, Germany) and RNA integrity was verified (2100 Bioanalyzer, Agilent Technologies, Santa Clara, CA). An Agilent Custom *P. gingivalis* Gene Expression Microarray (8 × 15K format) was designed (IMGM, Martinsried, Germany) by using the online tool EARRAY (http://earray.chem.agilent.com/, Agilent Technologies). Probe information regarding coding sequences of the relevant *P. gingivalis* transcriptome was retrieved from the NCBI reference sequence NC_002950.2 (http://www.ncbi.nlm.nih.gov/genome/714?project_id=57641). Before reverse transcription-in vitro transcription (RT-IVT) reaction (Applied Biosystems), the total RNA samples (500 ng) were spiked with *in vitro* synthesized polyadenylated transcripts (One-Color RNA Spike-In Mix, Agilent Technologies), which served as an internal labeling control for linearity, sensitivity and accuracy. The spiked total RNA was reverse transcribed into cDNA and then converted into labeled cRNA by *in vitro* transcription (Quick-Amp Labeling Kit One-Color, Agilent Technologies) incorporating Cyanine-3-CTP. Following cRNA clean-up and quantification, 0.6 μg of each Cyanine-3-labeled cRNA sample was fragmented and hybridized

© 2014 John Wiley & Sons A/S. Published by John Wiley & Sons Ltd

at 65°C for 17 h using One-Color-based hybridization (Gene Expression Hybridization Kit, Agilent Technologies). Fluorescent signal intensities were detected with Scan Control A.8.4.1 Software (Agilent Technologies) using the Agilent DNA Microarray Scanner. The software tools Feature Extraction 10.7.3.1, GeneSpring GX 12 (Agilent Technologies), Spotfire Decision Site 9.1.2 (TIBCO, Palo Alto, CA), and Excel 2007 were used for quality control, statistical data analysis, gene ontology annotation and visualization. Welch's approximate unpaired *t*-test assuming unequal variance was applied to the comparison of the different groups. The resulting *P*-value was corrected for multiple testing using the correction of Benjamini & Hochberg (1995). The extent and direction of differential expression between the groups was determined by calculating a fold change (FC) value. The averaged normalized signal values were transformed from the log2 to the linear scale and their ratio was calculated. For the identification of significantly differentially expressed RNAs, the FDR-adjusted *P*-value (corrected *P*-value) in addition to an absolute FC ≥ 2 or 1.5 was applied, together with a significance level of corrected *P*-value ≤ 0.05.

Quantitative reverse transcription-polymerase chain reaction

RNA was extracted from 4×10^8 cultured *P. gingivalis* cells using the GeneMATRIX Universal RNA Purification Kit (EURx) with modified lysis step. Before this step, RNA stabilization using RNAprotect Bacteria Reagent (Qiagen) was applied. Harvested bacterial cells were re-suspended in 0.1 ml 10 mM Tris–HCl buffer, pH 8.0, containing 140 mM NaCl, 1 mM EDTA, 1% Triton X-100, 15 mg ml^{-1} lysozyme and 55 mU proteinase K and incubated at room temperature for 15 min with continuous vigorous shaking (750 rpm). RNA concentration was determined spectrophotometrically using a NanoPhotometer (Implen, Munich, Germany). Before RNA integrity verification with the Agilent 2100 Bioanalyzer, samples were treated with DNase I (Thermo Scientific, Waltham, MA). Reverse transcription (RT) reaction was performed using 1 μg of RNA and the RevertAid Premium Reverse Transcriptase kit (Thermo Scientific).

Quantitative PCR (qPCR) was carried out using a Stratagene Mx3005P® QPCR System instrument (Agilent Technologies) and the SensiFast™ SYBR Lo-Rox Kit (Bioline, Taunton, MA). Amplification reactions consisted of an initial denaturation at 95°C for 10 min, 40 cycles of denaturation at 95°C for 30 s, primer annealing at 60°C for 30 s, and extension at 72°C for 1 min. The quality of PCR products was monitored using post-PCR melting curve analysis. Relative quantification of respective genes was determined in comparison with a *P. gingivalis 16S rRNA* gene (gene ID: 2552647) as a reference using the $\Delta\Delta C_t$ method. All samples were run in triplicate for the target and reference genes. No-template controls were included on each reaction plate to check for contamination. Negative controls consisting of untranscribed RNA (no-RT controls) were performed for each RNA extraction to check for genomic DNA contamination. All primers used in this study are listed in Table 1.

Plasmid construction and overexpression of recombinant PgFur protein variants

Three different types of expression plasmids for overexpression of His-tagged and untagged PgFur protein variants (Fig. 1) were constructed using the pTriEx-4 vector (Novagen Merck Millipore, Darmstadt, Germany) and primers listed in Table 1. All PgFur protein variants were overexpressed overnight in *E. coli* Rosetta (DE3) strain (Novagen) at 16°C and protein expression levels were analysed using SDS–PAGE as described previously (Olczak *et al.*, 2008).

Searching and clustering Fur homologs

To collect a comprehensive, non-redundant and reliable set of Fur homologs, at first we searched locally the Conserved Domain Database (Marchler-Bauer *et al.*, 2013) with 8,661,584 amino acid sequences annotated in 2770 completely sequenced archaeal and bacterial genomes downloaded from the GenBank database (www.ncbi.nlm.nih.gov). Next, we extracted sequences that showed the first hit with an E-value < 0.001 to ferric uptake regulator domains annotated as 223806 (COG0735), 201817 (pfam01475), 133478 (cd07153), 236527 (PRK09462) or 183251 (PRK11639). The first three domains also showed significant similarity with $E \leq 3E\text{-}13$ to the Fur sequence from *P. gingivalis*. The obtained set of 5285 sequences was subjected to clustering analysis performed in CLANS (Cluster Analysis of Sequences) software (Frickey & Lupas, 2004), which visualizes

© 2014 John Wiley & Sons A/S. Published by John Wiley & Sons Ltd

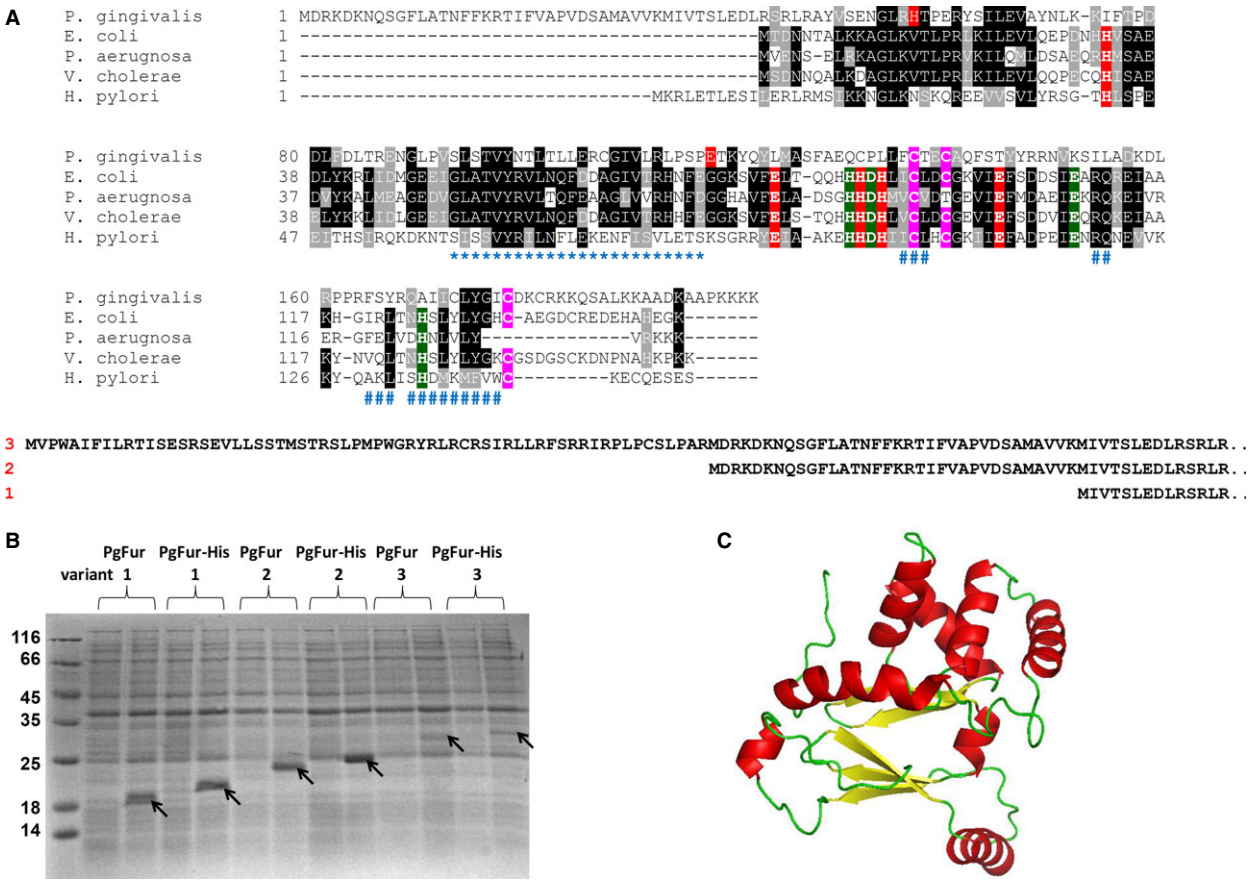

Figure 1 Analysis of amino acid sequence, homology modeling of PgFur three-dimensional structure and overexpression of PgFur protein variants. (A) Amino acid sequences were aligned using the CLUSTALW2 program with the default alignment parameters. Metal-binding S1 is marked in green, metal-binding S2 in red, structural Zn^{2+}-binding site in pink, DNA-binding helix with *, and dimer interface with #. The PgFur sequence revealed ferric-uptake regulator domain (IPR002481) in the range of 53–150 amino acids (aa) and winged helix-turn-helix DNA-binding domain (IPR011991) in the range of 46–122 aa (in InterProScan search). Potential Fur variant 1 (the longest predicted open reading frame), variant 2 (identified in W50 and JCVI SC001 strains, and clinical strains isolated from subgingival plaque biofilm or oral cavity) and variant 3 (identified in W83, A7436, and TDC60 strains) differ in their predicted N-terminal regions. (B) Sodium dodecyl sulfate–polyacrylamide gel electrophoresis demonstrating overexpression efficiency of PgFur variants 1–3. (C) The modeling was performed using the Web-based homology modeling server Phyre 2 using the following templates: 4I7H (PerR from *Streptococcus pyogenes*), 2FE3 (PerR from *Bacillus subtilis*), 2XIG (Fur from *Helicobacter pylori*), 4ETS (Fur from *Campylobacter jejuni*), 2O03 (FurB from *Mycobacterium tuberculosis*) and 1MZB (Fur from *Pseudomonas aeruginosa*), followed by additional refinement using ModRefiner.

BLAST pairwise sequence similarities in either two-dimensional or three-dimensional space. Based on this result, we excluded two outliers (probably false positives) and a clearly separated coherent set of 785 sequences, which most likely represented zinc uptake regulators (Zur). The final set included 4498 sequences, which were subjected to further studies. To automatically detect clusters of sequences, we applied the slowest but more effective 'convex' approach assuming the standard deviation = 0.8 and the minimum number of sequences per cluster = 2.

Phylogenetic analyses

Five *Porphyromonas* sequences, which created a separate cluster in CLANS analyses, together with sequences forming cluster 4 and overlapping the *Porphyromonas* cluster were used in phylogenetic studies. The amino acid alignment was obtained in MAFFT v7.130b using slow and accurate algorithm L-INS-i with 1000 cycles of iterative refinement (Katoh & Standley, 2013) and were edited manually in JalView (Waterhouse *et al.*, 2009) to remove poorly aligned sites. The final alignment included 131 sites and 470 sequences.

© 2014 John Wiley & Sons A/S. Published by John Wiley & Sons Ltd

To infer phylogenetic trees, we applied three approaches: Bayesian analysis in MrBayes 3.2.1 (Ronquist *et al.*, 2012) as well as maximum likelihood analyses in TreeFinder (Jobb *et al.*, 2004) and more-PhyML 1.14 (Criscuolo, 2011) based on PhyML 3.0 (Guindon *et al.*, 2010). In MrBayes analysis, we assumed the mixed+I+Γ(5) model and two independent runs starting from random trees, each using 18 Markov chains. Trees were sampled every 100 generations for 3,000,000 generations. In the final analysis, to calculate a posterior consensus, we selected trees from the last 892,000 generations that reached the stationary phase and convergence. In TreeFinder we applied a search depth set to 2 and the LG+F+I+Γ(5) substitution model as suggested by this program's Propose Model module. The tree inferred with (more)PhyML was based on the LG+I+Γ(5) substitution model as found in ProtTest 3.2 (Darriba *et al.*, 2011). The best heuristic search algorithm, nearest neighbor interchanges and subtree pruning and re-grafting, was applied in the (more)PhyML approach. To assess the significance of particular branches, non-parametric bootstrap analyses were performed on 100 replicates for TreeFinder and PhyML methods. Additionally, we applied the approximate likelihood ratio test based on a Shimodaira–Hasegawa-like procedure in morePhyML (Anisimova & Gascuel, 2006) and the Local Rearrangements–Expected Likelihood Weights method in TreeFinder.

Construction of PgFur three-dimensional protein structure

The modeling of the three-dimensional structure of PgFur was performed using the Web-based homology modeling server Phyre 2 (http://www.sbg.bio.ic.ac.uk/phyre2) using the following templates: 4I7H (PerR from *Streptococcus pyogenes*), 2FE3 (PerR from *Bacillus subtilis*), 2XIG (Fur from *H. pylori*), 4ETS (Fur from *C. jejuni*), 2O03 (FurB from *Mycobacterium tuberculosis*) and 1MZB (Fur from *Pseudomonas aeruginosa*). The resulting protein model was refined using ModRefiner (http://zhanglab.ccmb.med.umich.edu/ModRefiner/) and evaluated using PSVS online server (PROCHECK, Verify3, MolProbity, ProSA; http://psvs-15-dev.nesg.org/). The best model was selected on the basis of overall G-factor and Ramachandran Plot scores and further analysed using Verify3D (http://nihserver.mbi.ucla.edu/Verify_3D/), and ERRAT (http://nihserver.mbi.ucla.edu/ERRATv2/). The protein model was visualized using PyMOL software (The Open-Source PyMOL Molecular Graphics System Version 0.99r6 Schrödinger, LLC Schrodinger, New York, NY, USA).

RESULTS

Analysis of amino acid sequence and protein structure of *P. gingivalis* Fur

Similar to other bacteria, *P. gingivalis* possesses a putative homolog to the *fur* gene (e.g. PG0465 from W83 strain, PGN_1503 from ATCC 33277 strain, PGTDC60_1582 from TDC60 strain). Our preliminary experimental analyses of recombinant PgFur composed of 166 amino acid residues (PgFur variant 1, Fig. 1A) raised questions of its functional form. We have already analysed His-tagged and chitin-binding domain-tagged forms of this protein variant (data not shown). However, the protein comprising His-tag or that obtained after chitin-binding domain cleavage was highly unstable, resulting in significant aggregation, which raised the question whether the recombinant PgFur was active and functional. Therefore, in this study we thoroughly analysed amino acid sequences of PgFur deposited in databases, including data obtained from clinical strains, as well as analysing putative translation starting sites (Fig. 1A). It seems that the truncated version of the open reading frame (ORF) encoding PgFur (166 amino acid residues in length, PgFur variant 1) could be initially deposited in databases (e.g. AAF89746 from A7436 strain; AAQ65662 from W83 strain; BAK25731 from TDC60 strain; YP_001929619 from ATCC 33277 strain). Subsequently, the longer version of the ORF encoding PgFur (200 amino acid residues in length, PgFur variant 2) was proposed (e.g. EIW94221 from W50 strain; EOA10344 from JCVI SC001 strain and several others identified in clinical strains). We also identified an additional putative ORF encoding a potential product with the length of 263 amino acid residues (PgFur variant 3). We compared expression efficiency of all PgFur variants and found that variant 3 was expressed at a significantly lower level than variant 1 (the latter previously characterized in our laboratory) and variant 2 (Fig. 1B). Taking into account all the above-mentioned data, the functional form of PgFur still needs to be experimentally verified.

© 2014 John Wiley & Sons A/S. Published by John Wiley & Sons Ltd

Comparison of PgFur to its homologs identified in other bacteria shows the presence of motifs such as a DNA-binding domain or metal-binding sites, but also significant differences in their amino acid sequences (Fig. 1A). Fur proteins are usually rich in histidine residues, which may be engaged in binding of iron or other metals. In contrast, PgFur possesses only one histidine residue. Metal binding may also be performed by CXXCG or CP motifs, which are involved in heme binding in regulatory proteins, and these motifs are present in the C-terminal region of PgFur. To analyse the three-dimensional structure of PgFur, a computational approach was applied using amino acid sequences of PgFur and its homologous proteins belonging to a wide Fur family. Although N- and C-terminal regions of the resultant PgFur structure did not model well, the overall protein structure was similar to bacterial proteins belonging to this family (Fig. 1C).

Fur homologs and their clustering

Extensive and thorough searches for Fur homologs revealed the substantial number of 4498 sequences encoded in 2280 completely sequenced archaeal and bacterial genomes. Fur homologs are present in almost all the main prokaryotic groups (Table 2) with the exception of Nanoarchaeota, Korarchaeota and Armatimonadetes, but are represented by single genomes in the database. It indicates that this protein family is widely distributed in prokaryotes and must fulfill important functions. Nevertheless, there are some genomes that do not possess *fur* genes. The loss of these genes happened during the genome reduction process in many endosymbionts and parasites strictly associated with their host, e.g. *Anaplasma*, *Buchnera*, *Carsonella*, *Chlamydia*, *Ehrlichia*, *Hodgkinia*, *Mycoplasma*, *Nanoarchaeum*, *Phytoplasma* and *Rickettsia*. This indicates that Fur function is not essential, especially in specific environments that are rich in nutrients. Furthermore, no homolog was detected in different lineages of free-living Archaea (e.g. *Haloarcula*, *Halobacterium*, *Ignicoccus*, *Methanocaldococcus*, *Methanosarcina* and *Pyrococcus*). More than half of genomes (1216) encode more than one Fur homolog. An extreme number is observed in the cyanobacterium *Acaryochloris marina* MBIC11017 with as many as 14 paralogs.

The analysis performed on 4498 Fur homologs distinguished 24 clusters containing more than 10 sequences and 11 clusters comprising more than 100 sequences (Fig. 2). The clusters are characterized by different taxonomic distributions although many clusters were dominated by one taxonomic group (see Supporting information, Fig. S1). The most numerous were Firmicutes, present in eight clusters. γ-Proteobacteria dominated in one cluster and in two clusters they were the only members. Tenericutes also formed two of their own clusters and Actinobacteria had a

Table 2 Number and per cent of genomes in a given group with at least one homolog to Fur protein

Main group	Number of genomes		
	With Fur homolog	All in database	%
Acidobacteria	8	8	100
Actinobacteria	282	283	100
α-Proteobacteria	184	250	73
Aquificae	12	12	100
Bacteroidetes	78	99	79
β-Proteobacteria	146	160	91
Caldiserica	1	1	100
Saccharibacteria	1	1	100
Chlamydiae	2	106	2
Chlorobi	11	11	100
Chloroflexi	19	19	100
Chrysiogenetes	1	1	100
Cloacimonetes	1	1	100
Crenarchaeota	38	45	84
Cyanobacteria	74	75	99
Deferribacteres	4	4	100
Deinococcus-Thermus	20	20	100
δ-Proteobacteria	60	61	98
Dictyoglomi	2	2	100
Elusimicrobia	1	1	100
ε-Proteobacteria	105	105	100
Euryarchaeota	28	99	27
Fibrobacteres	2	2	100
Firmicutes	535	563	95
Fusobacteria	7	8	88
γ-Proteobacteria	541	570	94
Gemmatimonadetes	1	1	100
Ignavibacteriae	2	2	100
Nitrospirae	4	4	100
Planctomycetes	7	7	100
Spirochaetes	44	45	98
Synergistetes	5	5	100
Tenericutes	37	80	46
Thaumarchaeota	1	6	17
Thermobaculum	1	1	100
Thermodesulfobacteria	2	2	100
Thermotogae	17	17	100
Unclassified Archaea	1	2	50
Verrucomicrobia	4	4	100

© 2014 John Wiley & Sons A/S. Published by John Wiley & Sons Ltd

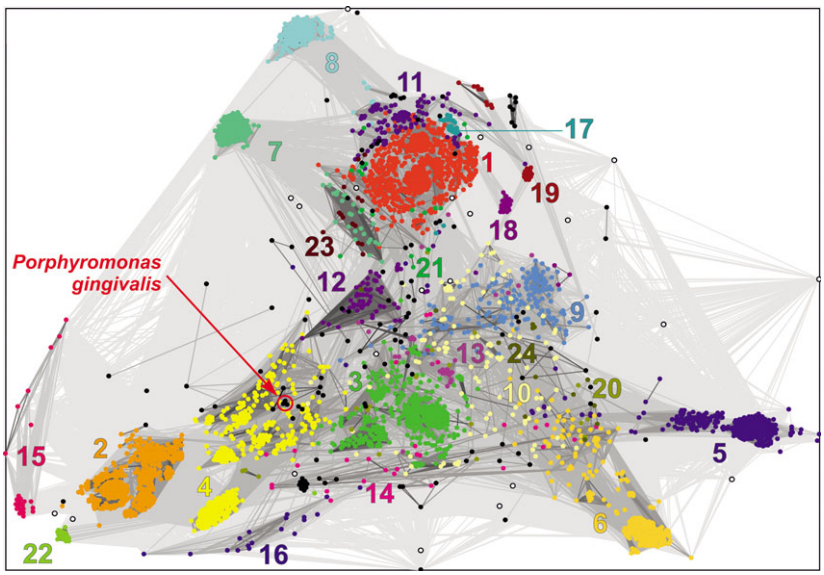

Figure 2 Cluster analysis of 4498 Fur homologs performed using CLANS software. Analysed sequences are represented by vertices connected by edges reflecting attractive forces proportional to the negative logarithm of the hidden subgroup problem (HSP) 's *P*-value. The grayness intensity of the connections is proportional to these forces. Recognized clusters containing more than 10 sequences were marked with different colors and numbered. White circles represent unclustered sequences. The location of *Porphyromonas gingivalis* sequences is indicated by an arrow.

large presence in two clusters. The presence of many separate clusters with domination by one group indicates rapid differentiation of the Fur family into various subgroups and further expansion in one taxonomic clade. Bacteroidetes, to which *P. gingivalis* belongs, were members of four clusters (1, 4, 9 and 21) with weak to moderate domination (2–51%). In addition, they created two small clusters, with two and five sequences, respectively. The five-sequence cluster included exclusively *Porphyromonas* sequences, two from *P. asaccharolytica* DSM 20707, and one from three *P. gingivalis* strains: ATCC 33277, TDC60 and W83. This cluster was located within the huge cluster 4 (Fig. 2), which in addition to Bacteroidetes (17%), included many representatives of α-Proteobacteria (37%), ε-Proteobacteria (24%), δ-Proteobacteria (12%) and other groups, each with a contribution of <3% (Fig. S1). For further studies we selected the five *Porphyromonas* sequences and all members of cluster 4, in total 470 sequences.

Phylogenetic relationships of selected Fur homologs

Phylogenetic trees obtained by different methods gave very similar topologies. Figure 3 presents the general phylogram inferred in morePhyML, whereas the supplementary Fig. S2 (see Supporting information) includes the detailed MOREPHYML cladogram with annotation and taxonomic affiliation of sequences as well as support values calculated in four approaches. Despite the quite short alignment and sequence variation, the trees are quite well resolved and many significantly supported groups can be distinguished. Clear monophyletic clades were created by α-Proteobacteria, ε-Proteobacteria, Spirochaetes, Aquificae, Planctomycetes, Chlorobi and Ignavibacteriae. However, sequences of δ-Proteobacteria were separated into three clades. Two of them also clustered representatives of other main bacterial groups (Fig. 3). Although these groupings were not always significantly supported, the close affiliations between δ-Proteobacteria with Nitrospirae, Acidobacteria and Thermodesulfobacteria were recently recovered by the maximum likelihood tree based on 24 conserved genes representing over 3000 genomes (Lang *et al.*, 2013). Therefore it seems that these connections represent true phylogenetic relationships. Three other δ-Proteobacteria from the *Bdellovibrio* genus clustered significantly by one method with ε-Proteobacteria, which may represent a probable horizontal gene transfer between ancestors of these lineages.

© 2014 John Wiley & Sons A/S. Published by John Wiley & Sons Ltd

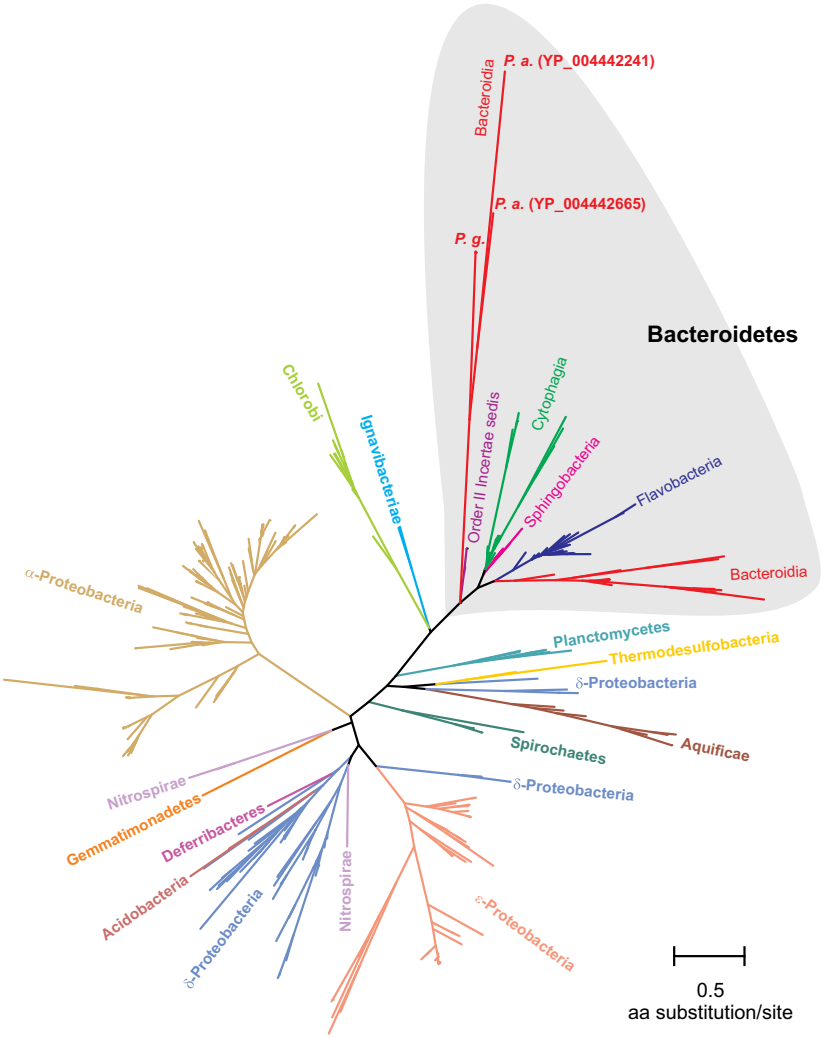

Figure 3 Phylogram for 470 Fur homologs inferred in MOREPHYML. Main bacterial groups are indicated in different colors. Five *Porphyromonas* sequences, two from *P. asaccharolytica* DSM 20707 (*P. a.*), and one from each of the three *P. gingivalis* strains ATCC 33277, TDC60 and W83 (*P. g.*) create a distinct, highly diverged clade.

Although the whole Bacteroidetes clade obtained rather moderate support, it created a distinct monophyletic group (Fig. 3). Three subgroups of Bacteroidetes – Flavobacteria, Sphingobacteria and Cytophagia – were also well defined with moderate to high support values. Five *Porphyromonas* sequences, two from *P. asaccharolytica* DSM 20707 and one from each of three *P. gingivalis* strains, ATCC 33277, TDC60 and W83, were clustered with very high support values but were separated from other members of their Bacteroidia subgroup. Interestingly, the sequences were the most diverged in the whole set. This suggests that some substantial changes probably happened in the functioning of the *Porphyromonas* Fur proteins in comparison to other Fur homologs. The recognized sequences could acquire substantial mutations, which forced appropriate changes in Fur proteins. Alternatively, these proteins evolved to bind other regulatory regions and in consequence to regulate other types of genes. Such functional flexibility of Fur proteins and their involvement in many various cellular processes has been widely reported (Lee & Helmann, 2007). The functional differentiation probably concerns two paralogs from *P. asaccharolytica* DSM 20707. One of them (YP_004442241) was subjected to an extremely high substitution rate, several times greater than in other sequences (Fig. 3). The paralogs found in 37 studied genomes represent recent duplications that happened in one genomic lineage or ancient events that occurred before divergence of several lineages (Fig. S2).

© 2014 John Wiley & Sons A/S. Published by John Wiley & Sons Ltd

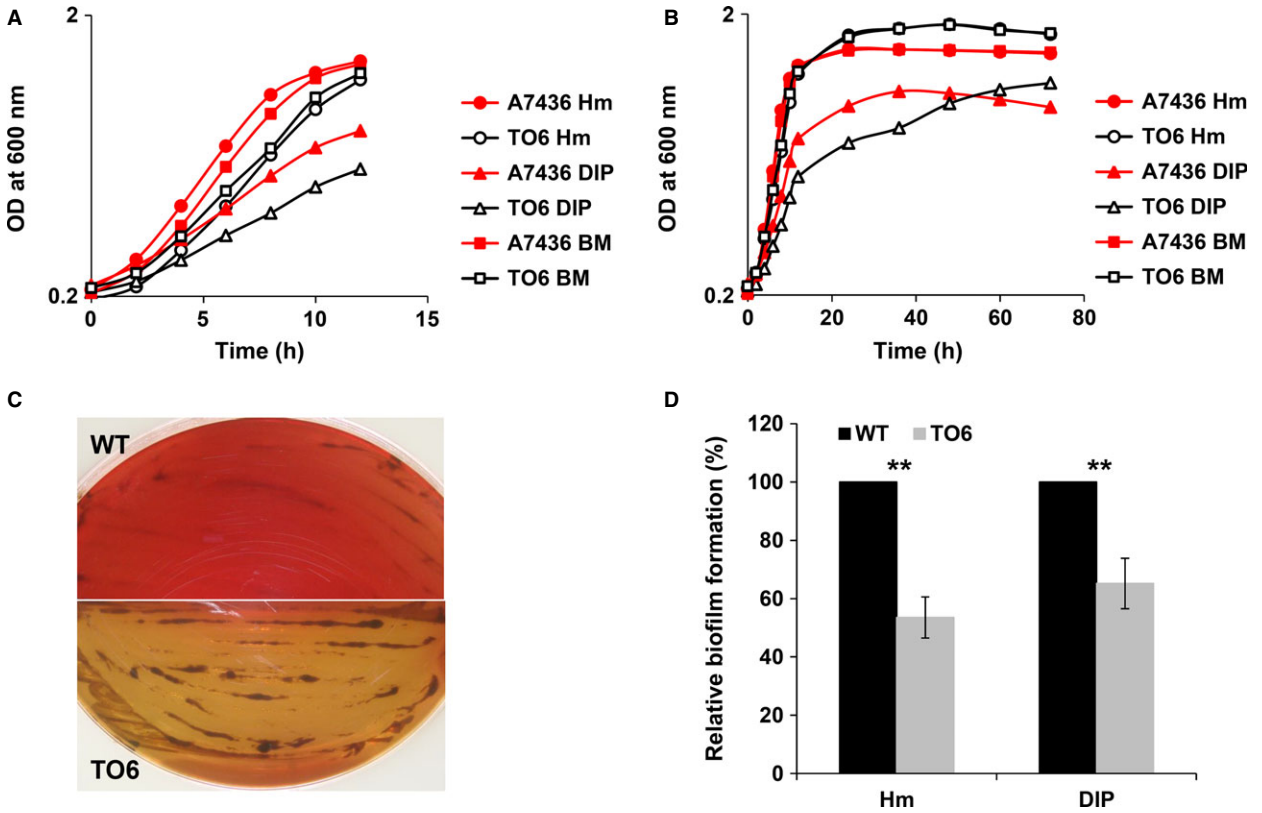

Figure 4 Phenotypic characterization of *Porphyromonas gingivalis fur* mutant strain. The *P. gingivalis* wild-type (WT, A7436) and *fur* mutant (TO6) strains were grown in liquid medium (A, B) or on blood agar plates (C). Bacterial cultures were started at optical density at 600 nm (OD_{600}) ~ 0.2 and the growth in liquid basal medium (BM), BM supplemented with heme (Hm) or dipyridyl (DIP) was monitored by measuring OD_{600} at the indicated time points. Growth on blood agar plates was visually observed for 72 h. Representative data out of three independent experiments with similar tendency are shown. (D) Biofilm was formed in basal medium supplemented with heme (Hm) or dipyridyl (DIP) for 24 h and analysed using crystal violet staining. Data are shown as mean ± standard deviation from three independent experiments performed in triplicate. $^{**}P < 0.01$.

Phenotypic characterization of *P. gingivalis fur* mutant strain

Although PgFur shows little amino acid sequence similarity to other Fur proteins, it has been shown that it may partially complement the functional activity of *E. coli* Fur (Olczak *et al.*, 2005). To gain more insight into the role played by Fur in *P. gingivalis*, we first constructed a *fur* mutant strain (TO6). As demonstrated by microarray analysis, inactivation of the *P. gingivalis fur* gene did not cause increased expression of the downstream genes (data not shown). Growth phenotype of the mutant strain was subsequently analysed using bacteria grown in liquid or solid culture media. Although slightly retarded growth was observed during the early growth phase (Fig. 4A), the TO6 strain produced higher bacterial biomass after prolonged growth compared with the wild-type strain (Fig. 4B). When bacteria were grown under iron and heme starvation, lower growth rates for the *fur* mutant strain were observed for a longer time, suggesting the importance of PgFur for bacterial growth under these conditions. When bacteria were grown on blood agar plates for a prolonged time, higher hemolytic activity of the mutant strain was observed compared with the wild-type strain (Fig. 4C). In contrast, the TO6 strain exhibited a significantly lower tendency to form homotypic biofilm on abiotic surfaces compared with the wild-type strain (Fig. 4D).

Invasion of host cells

To examine the general effect of the *fur* gene on *P. gingivalis* virulence, the ability of the bacterium to adhere and invade selected host cells was examined. As shown in Fig. 5, the growth of the *P. gingivalis fur* mutant strain in co-cultures with host cells in media

© 2014 John Wiley & Sons A/S. Published by John Wiley & Sons Ltd

designated for epithelial cells or macrophages resulted in a lower number of the TO6 cells compared with the wild-type cells. This suggests that PgFur is important for growth under low-iron/heme conditions, maintained *in vivo* by host iron- and heme-sequestering proteins present in culture media supplemented with serum. Importantly, inactivation of the *fur* gene caused a significant decrease in adherence and ability to invade and survive inside host cells, which suggests that the functional *fur* gene is required for *P. gingivalis* invasion, resulting in efficient infection of host cells.

Gene expression analysis of *P. gingivalis fur* mutant strain

To analyse expression of *P. gingivalis* genes at the global scale, we employed microarray analysis and compared the gene expression profile of the *fur* mutant strain to the wild-type strain, both grown in high-iron/heme media or starved of iron and heme. Our data demonstrate that the expression of 5 and 118 genes in the *fur* mutant strain significantly increased under high- and low-iron/heme conditions, respectively, whereas expression of 13 and 155 genes significantly decreased under the same conditions, respectively. Many of the differentially expressed genes had their potential products annotated as hypothetical proteins, conserved hypothetical proteins or proteins similar to proteins with uncharacterized functions (data not shown). In this study, we focused only on selected genes whose products have ascribed functions and might play a role in iron and heme acquisition, as well as expression of virulence factors. Surprisingly, no significant changes were found in expression of genes encoding the majority of

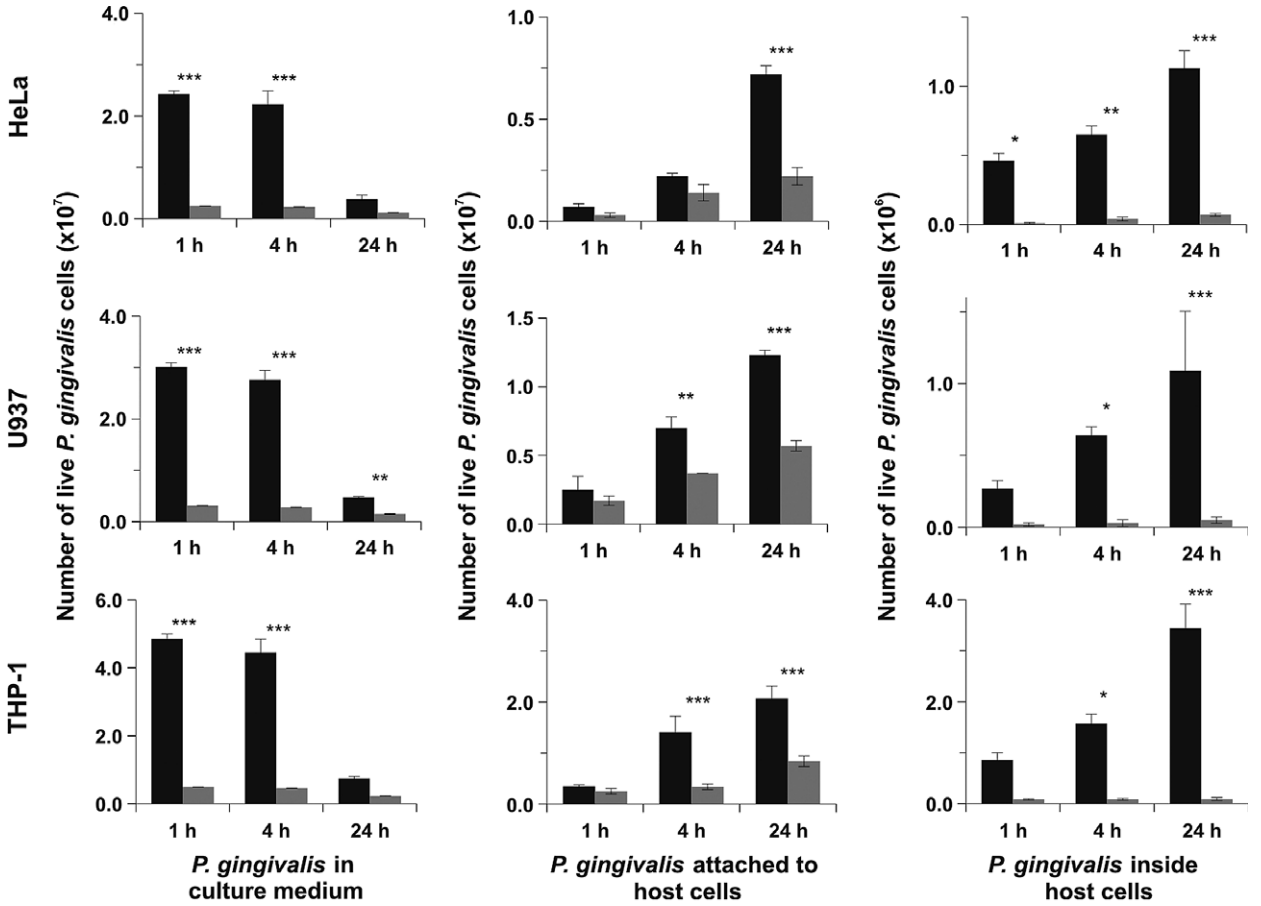

Figure 5 Analysis of invasion efficiency of *Porphyromonas gingivalis fur* mutant strain. The number of live *P. gingivalis* cells growing in the culture media, adhering to and invading epithelial HeLa cells or THP-1 and U937 cells differentiated to macrophages was enumerated using colony-forming assay (CFU) assay. Data are shown as mean ± standard deviation from three independent experiments performed in duplicate. $*P < 0.05$; $**P < 0.01$; $***P < 0.001$.

© 2014 John Wiley & Sons A/S. Published by John Wiley & Sons Ltd

typical iron or heme TonB-dependent outer-membrane receptors (data not shown). However, our data demonstrated changes in expression of transcripts encoding some hemagglutinins, gingipains and other proteases (Table 3). Verification of microarray data by qRT-PCR analysis and determination of transcript levels also after prolonged growth of starved bacteria using qRT-PCR showed that more significant changes were often observed (Fig. 6). It is worth noting that transcript levels, e.g. for *hagE(rgp)* and *dcp-2*, increased after prolonged growth under iron and heme starvation (Fig. 6), suggesting that also the growth phase may influence the expression of the examined genes. We also showed that two genes encoding glycosyltransferases, two genes encoding extracytoplasmic sigma factors (ECFs), and the gene encoding HtrA protein were expressed at lower levels in the absence of PgFur (Table 3).

As expected, *hmuY* gene expression in the wild-type strain increased significantly after passage to low-iron/heme conditions, as determined by microarray analysis (FC 156.31). A similar effect was determined by qRT-PCR, especially after persistent iron and heme starvation and prolonged growth (Fig. 7). Interestingly, we showed that inactivation of the *fur* gene resulted in slightly decreased *hmuY* gene expression under the conditions studied (Table 3). This effect was significantly higher after prolonged growth and iron/heme starvation (Fig. 7). In contrast, the expression of other *hmu* genes increased in the *fur* mutant strain (Table 3), suggesting differential expression of genes encoded by the *hmu* operon. It

Table 3 List of *Porphyromonas gingivalis* genes identified by microarray analysis that were differentially expressed in the *fur* mutant strain (TO6) compared with the wild-type strain (A7436)

	Fold change		
Locus ID (W83)	Hm	DIP	Annotation
PG0553	–1.51*	–3.21*	Extracellular protease
PG1326	–1.45*	–1.62*	Hemagglutinin
PG2024	–1.19	–1.45*	Hemagglutinin E, HagE, gingipain
PG1837	–1.56*	–1.39*	Hemagglutinin A HagA
PG0506	1.27	–1.53*	Arginine-specific cysteine proteinase, prtRII
PG1055	–1.63	–1.38*	Thiol protease, Tpr
PG0411	–1.70*	–1.59*	Hemagglutinin
PG0443	–2.19*	–1.64*	Hemagglutinin-like protein
PG1975	1.31	1.43*	Hemagglutinin C, HagC
PG0956	1.89	2.03*	M24/M37 family peptidase
PG1789	1.69	2.26*	Peptidyl-dipeptidase -2, Dcp-2
PG1551	1.31	–1.10	HmuY lipoprotein
PG1552	1.30	1.41*	TonB-dependent outer-membrane receptor, HmuR
PG1553	–1.37	1.87*	CobN/magnesium chelatase
PG1554	–1.36	2.39*	Hypothetical protein (ATPase)
PG1555	–1.52	2.70*	Hypothetical protein (MotA/TolQ/ExbB)
PG1556	–1.25	2.82*	Hypothetical protein
PG0719	–1.50	–1.92*	Sensor histidine kinase
PG0720	–1.31	–1.74*	DNA-binding response regulator
PG1431	1.00	–4.14*	LuxR family DNA-binding response regulator
PG1432	1.00	–2.86*	Sensor histidine kinase
PG0985	4.49*	–1.37*	ECF subfamily RNA polymerase sigma factor
PG1827	–1.46	–1.86*	ECF subfamily RNA polymerase sigma factor
PG0593	1.48	–1.94*	Periplasmic serine phosphatase, HtrA
PG0106	1.12	–2.51*	Glycosyltransferase
PG0920	–1.09	–1.84*	Glycosyltransferase group 2 family protein

Bacteria were grown in basal medium supplemented with hemin (Hm) or in basal medium without added hemin, but supplemented with dipyridyl (DIP); differentially expressed genes were identified using calculated fold change values of 2 and 1.5, together with a significance level of corrected $^*P \leq 0.05$.

© 2014 John Wiley & Sons A/S. Published by John Wiley & Sons Ltd

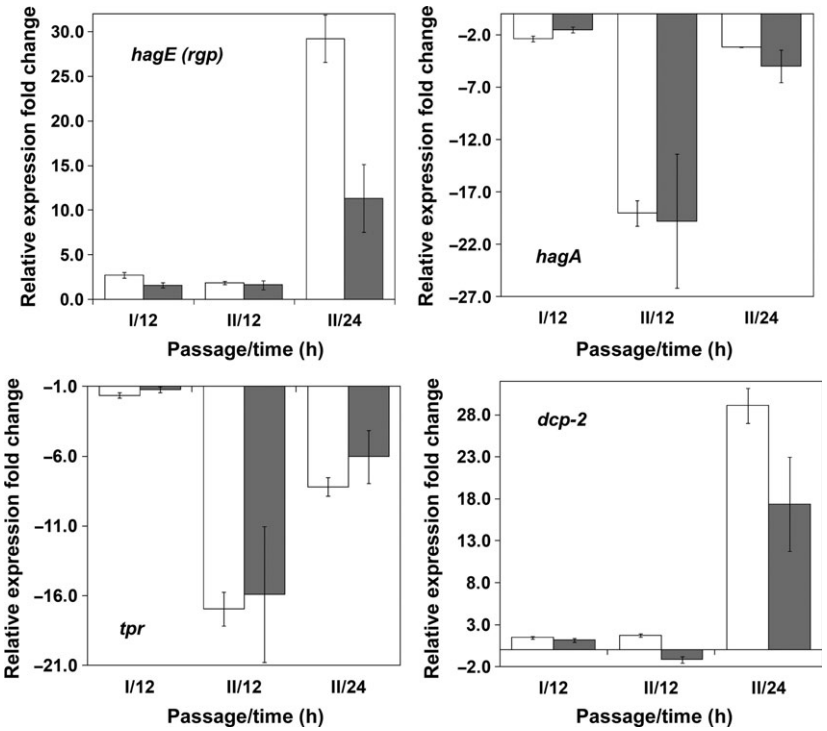

Figure 6 Expression of selected *Porphyromonas gingivalis* genes analysed by quantitative reverse transcription–polymerase chain reaction. The data are expressed as the relative quantity of the mRNA normalized to *16S rRNA* mRNA and are presented as mean ± standard deviation from three replicates.

has been shown that the expression of the *hmu* operon may be under the control of two-component system regulators responding to cell density (Hirano *et al.*, 2012). Here we demonstrated that expression of one such system, namely the system comprising PG1431 and PG1432, is downregulated in the absence of PgFur (Table 3). Another two-component system comprising PG0719 and PG0720, albeit at a lower level, is repressed in the *fur* mutant strain (Table 3).

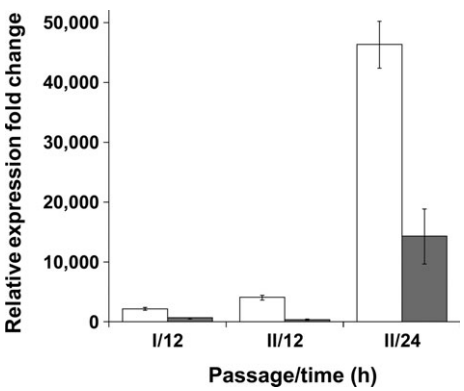

Figure 7 Expression of *Porphyromonas gingivalis hmuY* gene analysed by quantitative reverse transcription–polymerase chain reaction. The data are expressed as the relative quantity of the mRNA normalized to *16S rRNA* mRNA and presented as mean ± standard deviation from three replicates.

Results of the qRT-PCR analysis showed that the expression of *P. gingivalis fur* did change slightly until 12 h after passage into low-iron/heme conditions compared with high-iron/heme conditions (FC −1.61), corroborating data obtained from the microarray analysis (FC −1.56). In contrast, significant induction of *fur* gene expression was observed during the prolonged growth of bacteria under iron and heme starvation as determined by qRT-PCR (FC 5.52 after 24 h of second passage into BM+DIP). Based on these data, one may suggest that iron and heme levels, as well as growth phase, regulate *P. gingivalis fur* transcription.

Analysis of protein expression in *P. gingivalis fur* mutant strain

To investigate alterations in protein expression profiles as a result of the *fur* inactivation, the SDS PAGE

© 2014 John Wiley & Sons A/S. Published by John Wiley & Sons Ltd

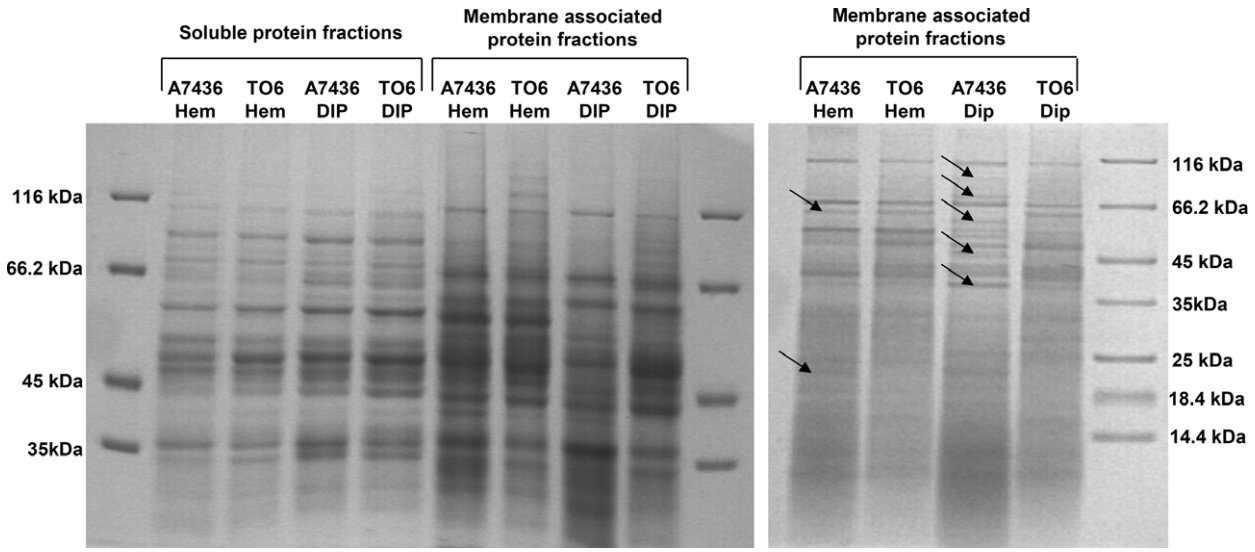

Figure 8 Representative images of sodium dodecyl sulfate–polyacrylamide gel electrophoresis Laemmli-based (left) and Schagger-based (right) gels. Samples prepared from the *Porphyromonas gingivalis* wild-type (WT, A7436) and *fur* mutant (TO6) strain, respectively, cultured in the presence of iron and heme (Hm) or in the presence of 160 μM dipyridyl (DIP). Arrows indicate bands showing changes in protein abundance.

Table 4 Summary of the mass spectrometry data demonstrating proteins differentially expressed in the *fur* mutant strain (TO6) compared with the wild-type strain (A7436)

Identified peptide sequence	Protein, in which the identified sequence can be found	Locus ID
YVAFR	Hemagglutinin	PG1326
	Peptidyl-dipeptidase-2, Dcp-2	PG1789
	Hemagglutinin E, HagE, gingipain	PG2024
	Hemagglutinin A, HagA	PG1837
YTAGVSPK	Hemagglutinin E, HagE, gingipain	PG2024
	Hemagglutinin A, HagA	PG1837
MWIAGDGGNQPAR	Hemagglutinin E, HagE, gingipain	PG2024
YDDFTFEAGK	Hemagglutinin E, HagE, gingipain	PG2024
KYTFTMR	Hemagglutinin E, HagE, gingipain	PG2024
AGMGDGTDMEVEDDSPASYTYTVYR	Hemagglutinin E, HagE, gingipain	PG2024
IWIAGQGPTKEDDYVFEAGK	Hemagglutinin E, HagE, gingipain	PG2024
MGSGDGTELTISEGGGSDYTYTVYR	Hemagglutinin E, HagE, gingipain	PG2024
APAPYQER	Hemagglutinin A, HagA	PG1837
TIDLSAYAGQQVYLAFR	Hemagglutinin A, HagA	PG1837
LYLDDVAVSGEGSSNDYTYTVYR	Hemagglutinin A, HagA	PG1837
VQGTWYQK	Hemagglutinin A, HagA	PG1837
NNTQIASGVTETTYRDPDLATGFYTYGVK	Hemagglutinin A, HagA	PG1837
VPIFAR	Thiol protease, Tpr	PG1055
NPWGVTEPTGDGVLSK	Thiol protease, Tpr	PG1055
DDGIFALR	Thiol protease, Tpr	PG1055
RDWVIHFDNMK	Thiol protease, Tpr	PG1055

patterns of whole-cell proteins of *P. gingivalis* A7436 and the *fur* mutant strain grown in the presence of iron and heme or under low-iron/heme conditions were compared. Since no significant differences were detected in whole-cell lysates, the whole-cell proteins were subjected to fractionation using ultracentrifugation. The most apparent differences were observed in protein contents of membrane fractions (Fig. 8). As

© 2014 John Wiley & Sons A/S. Published by John Wiley & Sons Ltd

shown in Table 4, inactivation of the *fur* gene resulted mostly in changes in the production of some hemagglutinins, gingipains and other proteases. However, based on this method, it is impossible to precisely identify respective peptides, because hemagglutinins and gingipains share identical amino acid sequences in several polypeptide regions.

DISCUSSION

Porphyromonas gingivalis expresses its transcriptome and proteome in response to external conditions (Xie *et al.,* 1997; Hirano *et al.*, 2012; Hovik *et al.*, 2012), so allowing production and utilization of a number of virulence-associated mechanisms. Among them, cell density in conjugation with iron and heme availability is an important environmental variable affecting the physiology of bacterial cells and is particularly important for the pathogenicity of *P. gingivalis*. Therefore, we have initiated studies on a putative Fur homolog in *P. gingivalis* with respect to its role in the regulation of iron/heme acquisition and the pathogen's virulence. Expression of proteins involved in iron and heme uptake, namely some hemagglutinins, hemolysins and proteases that are among the most important *P. gingivalis* pathogenicity factors, was regulated at least in part by PgFur. Although some transcripts encoding hemagglutinins and proteases were produced at lower levels, the proteins were found at higher amounts in the outer membrane. We hypothesize that in addition to differences in transcript levels, mobilization of some proteins to the outer membrane and subsequent protein accumulation as a compensatory mechanism for the lack of PgFur could be taken into consideration. Although results obtained by microarray analysis and qRT-PCR for the majority of genes are similar for bacteria starved under the same conditions and collected at the same time point, they should be viewed with caution. Similar to published data (Dallas *et al.*, 2005), we observed a small number of genes for which results from microarray analysis and qRT-PCR are different, for example for the *dcp-2* gene. This may be explained, at least in part, by the following reasons: (i) qRT-PCR is more sensitive in detecting relative changes, (ii) RNA fragmentation in microarray analysis might affect the binding sensitivity, (iii) different hybridization kinetics of the probe sets for each gene may exist, (iv) in both techniques different methods of data normalization are used.

Many responses in the bacterial cell are controlled by ECFs. We showed that production of transcripts encoding two ECFs, PG1827 and PG0985, as well as two genes encoding glycosyltransferases (PG0106 and PG0920), decreased in the absence of PgFur under low-iron/heme conditions. Since ECFs may be involved in the post-transcriptional regulation of gingipains, for example by affecting their glycosylation (Dou *et al.*, 2010), we propose a simple or two-layer regulatory network employing PgFur, which may regulate the expression of gingipains by controlling their transcription directly or through regulation of expression of ECFs. We also demonstrated that expression of the *htrA* gene (PG0593) decreased in the *fur* mutant strain grown under low-iron/heme conditions. HtrA is important for *in vivo* survival and virulence of *P. gingivalis* (Roy *et al.*, 2006; Yuan *et al.*, 2008). Mutation in the *htrA* gene altered expression of transcription regulators, including PG1431 (LuxR-family DNA-binding response regulator) (Yuan *et al.*, 2008), and knockout of *htrA* gene affected surface proteins, by decreasing expression of glycosyltransferases (Biswas & Biswas, 2005). Here we showed that also the gene encoding the PG1431 regulator exhibited decreased expression in the *fur* mutant strain grown under low-iron/heme conditions. It undoubtedly increases the complexity of the PgFur-based regulatory network.

We also demonstrated that *hmuY* expression under low iron/heme conditions is decreased in the absence of PgFur, especially after prolonged *P. gingivalis* growth. In contrast, expression of other *hmu* components increased in the *fur* mutant cells starved of iron and heme. Scott *et al.* (2013) have shown that the hypothetical protein PG1556 encoded by the *hmu* operon is regulated by a two-component system (HaeSR), comprising sensor histidine kinase (HaeS; PG0719) and a response regulator (HaeR; PG0720) with direct regulation involving binding of HaeR to a 5′ untranslated sequence upstream of the PG1553 (putative CobN/Mg chelatase) gene under low-heme conditions. Here we showed that regulation of *hmu* operon expression may involve a two-layer mechanism of regulation: one occurring with the direct involvement of the HaeSR two-component system, and the other occurring with indirect involvement of PgFur through regulation of HaeSR expression by PgFur. According to Scott *et al.* (2013), the HaeSR system may also regulate expression of gingipains

© 2014 John Wiley & Sons A/S. Published by John Wiley & Sons Ltd

and hemagglutinins, including Kgp and RgpA. We hypothesize that also in this case similar multi-layer regulation with the involvement of PgFur and other regulators may occur.

Porphyromonas gingivalis is a constituent of a multi-species biofilm within the gingival crevice and the periodontal pocket, which contributes to its persistence and increases the probability of periodontal tissue destruction. We demonstrated that this ability is regulated by PgFur, because the *fur* mutant strain forms significantly smaller homotypic biofilm structures. This effect, at least in part, may be caused by the decreased *hmuY* expression, because we have previously demonstrated that HmuY protein is important for *P. gingivalis* growth within biofilm structures (Olczak *et al.*, 2010). In addition, it has been shown that PG1431 (DNA-binding LuxR family response regulator) and PG1432 (sensor histidine kinase) from *P. gingivalis* W50 are upregulated during biofilm growth (Lo *et al.*, 2009). These genes are homologous to *P. gingivalis* ATCC 33277 FimR and FimS genes, respectively (Hayashi *et al.*, 2000; Wu *et al.*, 2007). We demonstrated that the decreased expression of this two-component system in the absence of PgFur may affect biofilm formation.

The initial event in the pathogenicity of *P. gingivalis* is its adherence to gingival epithelial cells. To accomplish this, the bacterium employs fimbriae, proteases, hemagglutinins and other proteins (Lamont *et al.*, 1995; Holt *et al.*, 1999). We demonstrate that *P. gingivalis* lacking PgFur exhibited significantly diminished ability to adhere to host cells, and most importantly to invade and survive inside epithelial cells and macrophages, suggesting that this protein is crucial for efficient infection. It is likely that the decreased expression of the two-component system (PG1431 and PG1432) in the absence of PgFur may influence invasion efficiency of host cells by *P. gingivalis*. However, because *P. gingivalis* A7436 strain, similar to W83, is one of the less fimbriated strains, other components, such as hemagglutinin domains, may mediate adhesion to host cells (Belanger *et al.*, 2012). Again, our data suggest multi-layer, complex regulation of genes expressing virulence factors in *P. gingivalis*, especially under low-iron/heme conditions, employing not only direct regulation of some genes by PgFur (so far not precisely identified), but also indirect PgFur regulation by influencing expression of other regulators. Therefore we propose that other mechanisms apart from direct negative regulation by PgFur, as well as the presence of other regulator/s acting in the *P. gingivalis* cell, should be taken into consideration.

ACKNOWLEDGEMENTS

We thank Dr Piotr Jakimowicz for performing MALDI TOF/TOF MS analysis. This work was supported in part by Wroclaw Research Center EIT+ under the project 'Biotechnologies and advanced medical technologies – BioMed' (POIG 01.01.02-02-003/08/00) financed by the European Regional Development Fund (Operational Program Innovative Economy, 1.1.2) and by Faculty of Biotechnology University of Wroclaw research projects 1496/M/WB/11 and 1013/S/WB/2013. The funders had no role in study design, data collection and analysis, or preparation of the manuscript.

REFERENCES

Anisimova, M. and Gascuel, O. (2006) Approximate likelihood-ratio test for branches: a fast, accurate, and powerful alternative. *Syst Biol* **55**: 539–552.

Belanger, M., Kozarov, E., Song, H., Whitlock, J. and Progulske-Fox, A. (2012) Both the unique and repeat regions of the *Porphyromonas gingivalis* hemagglutinin A are involved in adhesion and invasion of host cells. *Anaerobe* **18**: 128–134.

Benjamini, Y. and Hochberg, Y. (1995) Controlling the false discovery rate: a practical and powerful approach to multiple testing. *J R Stat Soc Series B Methodol* **57**: 289–300.

Benson, D.R. and Rivera, M. (2013) Heme uptake and metabolism in bacteria. *Met Ions Life Sci* **12**: 279–332.

Biswas, S. and Biswas, I. (2005) Role of HtrA in surface protein expression and biofilm formation by *Streptococcus mutans*. *Infect Immun* **73**: 6923–6934.

Bostanci, N. and Belibasakis, G.N. (2012) *Porphyromonas gingivalis*: an invasive and evasive opportunistic pathogen. *FEMS Microbiol Lett* **333**: 1–9.

Butcher, J., Sarvan, S., Brunzelle, J.S., Couture, J.F. and Stintzi, A. (2012) Structure and regulon of *Campylobacter jejuni* ferric uptake regulator Fur define apo-Fur regulation. *Proc Natl Acad Sci USA* **109**: 10047–10052.

Byrne, D.P., Potempa, J., Olczak, T. and Smalley, J.W. (2013) Evidence of mutualism between two periodontal pathogens: co-operative haem acquisition by the HmuY haemophore of *Porphyromonas gingivalis* and the cyste-

© 2014 John Wiley & Sons A/S. Published by John Wiley & Sons Ltd

ine protease interpain A (InpA) of *Prevotella intermedia*. *Mol Oral Microbiol* **28**: 219–229.

Craig, R.G., Yip, Y.K., So, M.K., Boylan, R.J., Socransky, S.S. and Haffajee, A.D. (2003) Relationship of destructive periodontal disease to the acute-phase response. *J Periodontol* **74**: 1007–1016.

Criscuolo, A. (2011) morePhyML: improving the phylogenetic tree space exploration with PhyML 3. *Mol Phylogenet Evol* **61**: 944–948.

Dallas, P.B., Gottardo, N.G., Firth, M.J. *et al.* (2005) Gene expression levels assessed by oligonucleotide microarray analysis and quantitative real-time RT-PCR – how well do they correlate? *BMC Genomics* **6**: 59.

Darriba, D., Taboada, G.L., Doallo, R. and Posada, D. (2011) ProtTest 3: fast selection of best-fit models of protein evolution. *Bioinformatics* **27**: 1164–1165.

Delany, I., Ieva, R., Alaimo, C., Rappuoli, R. and Scarlato, V. (2001) The iron-responsive regulator Fur is transcriptionally autoregulated and not essential in *Neisseria meningitides*. *J Bacteriol* **185**: 6032–6041.

Dian, C., Vitale, S., Leonard, G.A. *et al.* (2011) The structure of the *Helicobacter pylori* ferric uptake regulator Fur reveals three functional metal binding sites. *Mol Microbiol* **79**: 1260–1275.

Dou, Y., Osbourne, D., McKenzie, R. and Fletcher, H. (2010) Involvement of extracytoplasmic function sigma factors in virulence regulation in *Porphyromonas gingivalis*. *FEMS Microbiol Lett* **312**: 24–32.

Dubrac, S. and Touati, D. (2000) Fur positive regulation of iron superoxide dismutase in *Escherichia coli*: functional analysis of the *sodB* promoter. *J Bacteriol* **182**: 3802–3808.

Frickey, T. and Lupas, A.N. (2004) CLANS: a Java application for visualizing protein families based on pairwise similarity. *Bioinformatics* **20**: 3702–3704.

Gmiterek, A., Wojtowicz, H., Mackiewicz, P. *et al.* (2013) The unique *hmuY* gene sequence as a specific marker of *Porphyromonas gingivalis*. *PLoS One* **8**: e67719.

Graves, D.T., Jiang, Y. and Genco, C.A. (2000) Periodontal disease: bacterial virulence factors, host response and impact on systemic health. *Curr Opin Infect Dis* **13**: 227–232.

Griffen, A.L., Becker, M.R., Lyons, S.R., Moeschberger, M.L. and Leys, E.J. (1998) Prevalence of *Porphyromonas gingivalis* and periodontal health status. *J Clin Microbiol* **36**: 3239–3242.

Guindon, S., Dufayard, J.F., Lefort, V., Anisimova, M., Hordijk, W. and Gascuel, O. (2010) New algorithms and methods to estimate maximum-likelihood phylogenies: assessing the performance of PhyML 3.0. *Syst Biol* **59**: 307–321.

Guyodo, H., Meuric, V., Le Pottier, L. *et al.* (2012) Colocalization of *Porphyromonas gingivalis* with CD4+ T cells in periodontal disease. *FEMS Immunol Med Microbiol* **64**: 175–183.

Haffajee, A.D., Cugini, M.A., Tanner, A. *et al.* (1998) Subgingival microbiota in healthy, well-maintained elder and periodontitis subjects. *J Clin Periodontol* **25**: 346–353.

Hajishengallis, G. (2011) Immune evasion strategies of *Porphyromonas gingivalis*. *J Oral Biosci* **53**: 233–240.

Hantke, K. (2001) Iron and metal regulation in bacteria. *Curr Opin Microbiol* **4**: 172–177.

Hayashi, J., Nishikawa, K., Hirano, R., Noguchi, T. and Yoshimura, F. (2000) Identification of a two-component signal transduction system involved in fimbriation of *Porphyromonas gingivalis*. *Microbiol Immunol* **44**: 279–282.

Hernandez, J.A., Peleato, M.L., Fillat, M.F. and Bes, M.T. (2004) Heme binds to and inhibits the DNA-binding activity of the global regulator FurA from *Anabaena* sp. PCC 7120. *FEBS Lett* **577**: 35–41.

Hirano, T., Beck, D.A., Demuth, D.R., Hackett, M. and Lamont, R.J. (2012) Deep sequencing of *Porphyromonas gingivalis* and comparative transcriptome analysis of a LuxS mutant. *Front Cell Infect Microbiol* **2**: 79.

Holt, S.C., Kesavalu, L., Walker, S. and Genco, C.A. (1999) Virulence factors in *Porphyromonas gingivalis*. *Periodontol 2000* **20**: 168–238.

Hovik, H., Yu, W.H., Olsen, I. and Chen, T. (2012) Comprehensive transcriptome analysis of the periodontopathogenic bacterium *Porphyromonas gingivalis* W83. *J Bacteriol* **194**: 100–114.

Jobb, G., von Haeseler, A. and Strimmer, K. (2004) TREEFINDER: a powerful graphical analysis environment for molecular phylogenetics. *BMC Evol Biol* **4**: 18.

Katoh, K. and Standley, D.M. (2013) MAFFT multiple sequence alignment software version 7: improvements in performance and usability. *Mol Biol Evol* **30**: 772–780.

Kuboniwa, M. and Lamont, R.J. (2010) Subgingival biofilm formation. *Periodontol 2000* **52**: 38–52.

Laemmli, U.K. (1970) Cleavage of structural proteins during the assembly of the head of bacteriophage T4. *Nature* **227**: 680–685.

Lamont, R.J., Chan, A., Belton, C.M., Izutsu, K.T., Vasel, D. and Weinberg, A. (1995) *Porphyromonas gingivalis* invasion of gingival epithelial cells. *Infect Immun* **63**: 3878–3885.

© 2014 John Wiley & Sons A/S. Published by John Wiley & Sons Ltd

Lang, J.M., Darling, A.E. and Eisen, J.A. (2013) Phylogeny of bacterial and archaeal genomes using conserved genes: supertrees and supermatrices. *PLoS One* **8**: e62510.

Lee, J.W. and Helmann, J.D. (2007) Functional specialization within the Fur family of metalloregulators. *Biometals* **20**: 485–499.

Lo, A., Seers, C.A., Boyce, J. *et al.* (2009) Comparative transcriptomic analysis of *Porphyromonas gingivalis* biofilm and planktonic cells. *BMC Microbiol* **9**: 18.

Marchler-Bauer, A., Zheng, C., Chitsaz, F. *et al.* (2013) CDD: conserved domains and protein three-dimensional structure. *Nucleic Acids Res* **41**(D1): D348–D352.

Marsh, P.D. (2004) Dental plaque as a microbial biofilm. *Caries Res* **38**: 204–211.

Meurman, J.H., Sanz, M. and Janket, S.J. (2004) Oral health, atherosclerosis, and cardiovascular disease. *Crit Rev Oral Biol Med* **15**: 403–413.

Nakagawa, I., Inaba, H., Yamamura, T. *et al.* (2006) Invasion of epithelial cells and proteolysis of cellular focal adhesion components by distinct types of *Porphyromonas gingivalis* fimbriae. *Infect Immun* **74**: 3773–3782.

Olczak, T., Simpson, W., Liu, X. and Genco, C.A. (2005) Iron and heme utilization in *Porphyromonas gingivalis*. *FEMS Microbiol Rev* **29**: 119–144.

Olczak, T., Sroka, A., Potempa, J. and Olczak, M. (2008) *Porphyromonas gingivalis* HmuY and HmuR: further characterization of a novel mechanism of heme utilization. *Arch Microbiol* **183**: 197–210.

Olczak, T., Wojtowicz, H., Ciuraszkiewicz, J. and Olczak, M. (2010) Species specificity, surface exposure, protein expression, immunogenicity, and participation in biofilm formation of *Porphyromonas gingivalis* HmuY. *BMC Microbiol* **10**: 134.

Olczak, T., Maszczak-Seneczko, D., Smalley, J.W. and Olczak, M. (2012) Gallium(III), cobalt(III) and copper(II) protoporphyrin IX exhibit antimicrobial activity against *Porphyromonas gingivalis* by reducing planktonic and biofilm growth and invasion of host epithelial cells. *Arch Microbiol* **194**: 719–724.

Pecqueur, L., D'Autreaux, B., Dupuy, J. *et al.* (2006) Structural changes of *Escherichia coli* ferric uptake regulator during metal-dependent dimerization and activation explored by NMR and X-ray crystallography. *J Biol Chem* **281**: 21286–21295.

Pellicer, S., Gonzalez, A., Peleato, M.L., Martinez, J.I., Fillat, M.F. and Bes, M.T. (2012) Site-directed mutagenesis and spectral studies suggest a putative role of FurA from *Anabaena* sp. PCC 7120 as a heme sensor protein. *FEBS J* **279**: 2231–2246.

Pohl, E., Haller, J.C., Mijovilovich, A., Meyer-Klaucke, W., Garman, E. and Vasil, M.L. (2003) Architecture of a protein central to iron homeostasis: crystal structure and spectroscopic analysis of the ferric uptake regulator. *Mol Microbiol* **47**: 903–915.

Potempa, J., Sroka, A., Imamura, T. and Travis, J. (2003) Gingipains, the major cysteine proteinases and virulence factors of *Porphyromonas gingivalis*: structure, function and assembly of multidomain protein complexes. *Curr Protein Pept Sci* **4**: 397–407.

Ronquist, F., Teslenko, M., van der Mark, P. *et al.* (2012) MrBayes 3.2: efficient Bayesian phylogenetic inference and model choice across a large model space. *Syst Biol* **61**: 539–542.

Rosenstein, E.D., Greenwald, R.A., Kushner, L.J. and Weissmann, G. (2004) Hypothesis: the humoral immune response to oral bacteria provides a stimulus for the development of rheumatoid arthritis. *Inflammation* **28**: 311–318.

Roy, F., Vanterpool, E. and Fletcher, H.M. (2006) HtrA in *Porphyromonas gingivalis* can regulate growth and gingipain activity under stressful environmental conditions. *Microbiology* **152**: 3391–3398.

Schagger, H. (2006) Tricine-SDS-PAGE. *Nat Protoc* **1**: 16–22.

Scott, J.C., Klein, B.A., Duran-Pinedo, A., Hu, L. and Duncan, M.J. (2013) A two-component system regulates hemin acquisition in *Porphyromonas gingivalis*. *PLoS One* **8**: e73351.

Sheikh, M.A. and Taylor, G.L. (2009) Crystal structure of the *Vibrio cholerae* ferric uptake regulator (Fur) reveals insights into metal co-ordination. *Mol Microbiol* **72**: 1208–1220.

Simpson, W., Olczak, T. and Genco, C.A. (2000) Characterization and expression of HmuR, a TonB-dependent hemoglobin receptor of *Porphyromonas gingivalis*. *J Bacteriol* **182**: 5737–5748.

Smalley, J.W., Byrne, D.P., Birss, A.J. *et al.* (2011) HmuY haemophore and gingipain proteases constitute a unique synthrophic system of haem acquisition by *Porphyromonas gingivalis*. *PLoS One* **6**: e17182.

Vitkov, L., Krautgartner, W.D. and Hannig, M. (2005) Bacterial internalization in periodontitis. *Oral Microbiol Immunol* **20**: 317–321.

Waterhouse, A.M., Procter, J.B., Martin, D.M.A., Clamp, M. and Barton, G.J. (2009) Jalview version 2: a multiple sequence alignment and analysis workbench. *Bioinformatics* **25**: 1189–1191.

Wojtowicz, H., Guevara, T., Tallant, C. *et al.* (2009) Unique structure and stability of HmuY, a novel

© 2014 John Wiley & Sons A/S. Published by John Wiley & Sons Ltd

heme-binding protein of *Porphyromonas gingivalis*. *PLoS Pathog* **5**: e1000419.

Wojtowicz, H., Bielecki, M., Wojaczynski, J., Olczak, M., Smalley, J.W. and Olczak, T. (2013) *Porphyromonas gingivalis* HmuY haemophore binds gallium(III), zinc(II), cobalt(III), manganese(III), nickel(II), and copper(II) protoporphyrin IX but in a manner different to iron(III) protoporphyrin IX. *Metallomics* **5**: 343–351.

Wu, J., Lin, X. and Xie, H. (2007) *Porphyromonas gingivalis* short fimbriae are regulated by a FimS/FimR two-component system. *FEMS Microbiol Lett* **271**: 214–221.

Xie, H., Cai, S. and Lamont, R.J. (1997) Environmental regulation of fimbrial gene expression in *Porphyromonas gingivalis*. *Infect Immun* **65**: 2265–2271.

Yilmaz, O., Verbeke, P., Lamont, R.J. and Ojcius, D.M. (2006) Intercellular spreading of *Porphyromonas gingivalis* infection in primary gingival epithelial cells. *Infect Immun* **74**: 703–710.

Yuan, L., Rodrigues, P.H., Belanger, M., Dunn, W.A. Jr and Progulske-Fox, A. (2008) *Porphyromonas gingivalis htrA* is involved in cellular invasion and *in vivo* survival. *Microbiology* **154**: 1161–1169.

SUPPORTING INFORMATION

Additional supporting information may be found in the online version of this article at the publisher's web-site.

© 2014 John Wiley & Sons A/S. Published by John Wiley & Sons Ltd